Role of dimer interface in activation and desensitization in AMPA receptors

Jennifer Gonzalez[a], Mei Du[a], Kodeeswaran Parameshwaran[b], Vishnu Suppiramaniam[b], and Vasanthi Jayaraman[a,1]

[a]Center for Membrane Biology, Department of Biochemistry and Molecular Biology, Graduate School of Biomedical Sciences, University of Texas Health Science Center, Houston, TX 77030; and [b]Department of Pharmacal Sciences, Auburn University, Auburn, AL 36849

Edited by Jonathan A. Javitch, Columbia University College of Physicians and Surgeons, New York, NY, and accepted by the Editorial Board April 23, 2010 (received for review October 13, 2009)

The conversion of chemical to electrical signals by the AMPA receptors is the key step by which these proteins control cognitive and motor responses. Here, we have used luminescence resonance energy transfer (LRET) to gain insight into the conformational changes induced by glutamate binding in the agonist-binding domain in functional AMPA receptors expressed in oocytes and HEK-293 cells. The LRET-based distances indicate that the interface between the upper lobes of the agonist-binding domain within a dimer is in a decoupled state in the unligated Apo state of the receptor. Agonist binding results in the formation of the dimer interface in the open-channel form of the receptor. In the continued presence of glutamate when the receptor is primarily in the desensitized state, the dimer interface is decoupled, confirming that the decoupling of the dimer interface leads to channel closure. The LRET distances also indicate that the dimer interface is preformed before activation in the L484Y mutation and also is formed in the antagonist (ZK200775)-bound form of the AMPA receptor. These results suggests that, although the preformation of the interface is not sufficient to drive channel activation, it could play a role in the energetics of activation and hence modulation of the receptor by auxiliary proteins or small molecules.

allosteric mechanism | glutamate receptors | luminescence resonance energy transfer | structure-function

AMPA subtype of the ionotropic glutamate receptors are the primary mediators of fast excitatory synaptic signals in the central nervous system and play a critical role in processes such as learning and memory as well as in diverse neuropathologies, including epilepsy and ischemia (1–6). Glutamate binding to an extracellular domain in the receptors triggers a series of conformational changes that leads to the formation of a cation-selective transmembrane channel and subsequent desensitization. AMPA receptors are tetrameric proteins thought to assemble as a dimer of dimers (7–9). Each subunit is made up of an extracellular N-terminal domain and ligand-binding domain, three transmembrane segments with an ion-channel pore-lining loop, and an intracellular C-terminal segment. This modular nature of the AMPA receptors has allowed the determination of the crystal structures of extracellular components (7–16). Specifically, the structures of the isolated ligand-binding domain have provided invaluable insight into the conformational changes within the domain which in turn control and modulate the changes in the channel-forming transmembrane segments (7–15, 17).

One of the limitations of these isolated structures is that they do not feel the constraints placed on these extracellular domains by the transmembrane segments anchored in the membrane. This limitation is manifested in the intersubunit contacts and is clearly evident in the desensitized state of the receptor (9, 14). Biochemical investigations show that blocking desensitization and stabilizing the open-channel form with the L484Y mutation or using cyclothiazide promotes dimerization of the isolated ligand-binding domain (14). The structures of the isolated ligand-binding domain show that the tyrosine introduced at site GluR2-S1S2-L483Y (484 in GluR4) forms an intersubunit hydrogen bond with Leu748, thus stabilizing the dimer, and cyclothiazide binds to the dimer interface, stabilizing the intersubunit contacts (14). Conversely, destabilizing the dimer interface with the S754D mutations resulted in rapid desensitization (14), suggesting a decoupled interface in the desensitized state of the protein. However, the isolated ligand-binding domain crystal structure that corresponds to the desensitized state does not have a decoupled interface. A structure of the decoupled dimer interface at the D1 segment of the ligand-binding domain could be determined only by artificially decoupling the interface by introducing a disulfide bond deep in the interface of the dimer (Fig. 1) (9). This structure is thought to represent a state resembling desensitization because the corresponding full-length receptor with the disulfide mutation is found to be functionally desensitized.

Although the state of the dimer interface in the open and desensitized states could be investigated indirectly by correlating the structural investigations to the functional consequences, such a study has not been possible with the resting state, primarily because of the absence functional consequences. Hence, it currently is assumed that the dimer interface is preformed in the resting state based on the Apo state structures of the isolated ligand-binding domain (Fig. 1). While this article was in review, the structure of the full-length rat GluR2 subunit of AMPA receptor in complex with competitive antagonist ZK200775 was published (18). This structure shows that the antagonist stabilized the ligand-binding domain in a hyperextended form relative to the resting Apo state, and in this form the dimer interface was coupled, as shown by the presence of the interdimer contacts in the upper lobe of the agonist-binding domain within the dimer. Whether the antagonist-bound hyperextended form of the receptor represents the resting state of the protein is still unknown. Here we have used luminescence resonance energy transfer (LRET) measurements to obtain distance changes at the dimer interface in the presence of the transmembrane segments in the receptor expressed in oocytes and HEK-293 cells under conditions where it is primarily in the closed resting state, open-channel state, and desensitized state, as well as in the competitive antagonist ZK200775-bound form, thus allowing a direct determination of the state of the dimer interface in a functional receptor.

Author contributions: J.G., V.S., and V.J. designed research; J.G., M.D., K.P., and V.J. performed research; J.G., M.D., K.P., V.S., and V.J. analyzed data; and J.G. and V.J. wrote the paper.

The authors declare no conflict of interest.

This article is a PNAS Direct Submission. J.A.J. is a guest editor invited by the Editorial Board.

[1]To whom correspondence should be addressed. E-mail: vasanthi.jayaraman@uth.tmc.edu.

This article contains supporting information online at www.pnas.org/lookup/suppl/doi:10.1073/pnas.0911854107/-/DCSupplemental.

PHARMACOLOGY

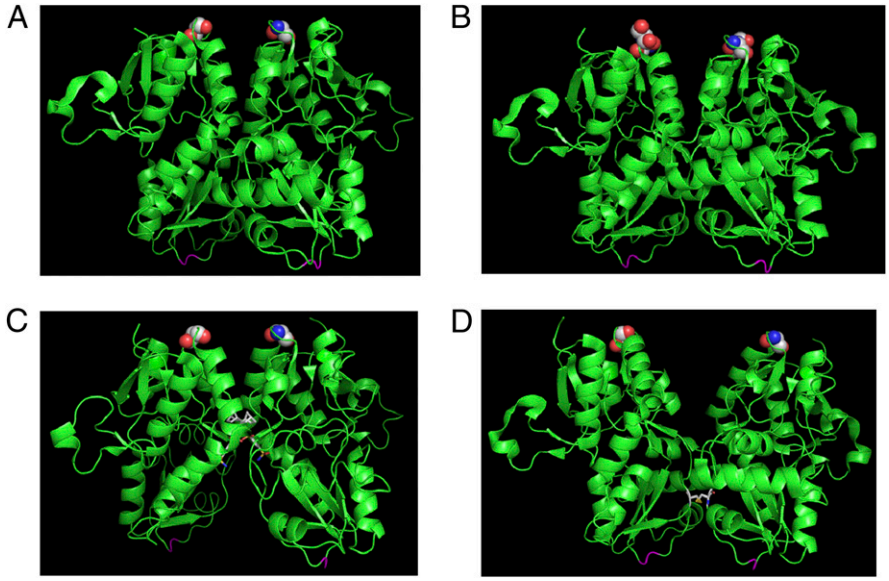

Fig. 1. Crystal structures of AMPA receptor ligand-binding domain (GluR2-S1S2) showing the dimer interface. The structures are (*A*) in the Apo state, (*B*) in the glutamate-bound state, (*C*) glutamate-bound in the presence of cyclothiazide, and (*D*) the S729C structure thought to represent the desensitized dimer interface. Residue 740 (741 in GluR4) in GluR2-S1S2, which was tagged with the donor:acceptor fluorophore in the LRET measurements, is highlighted as spheres, and the linker region where the transmembrane segments are attached is shown in magenta. All the structures show an intact dimer interface; the only structure that is different in terms of the interface, *D*, is shown in the GluR2-S1S2-S729C structure.

Results and Discussion

LRET Constructs and Electrophysiological Characterization. To perform the LRET investigations, we have modified the GluR4 subunit by deleting the N-terminal domain and mutating the accessible cysteines residues 426 and 529 to serines (ΔN*-GluR4). To probe and quantify the distance within the dimer, we have mutated the residues at sites 740, 741, and 742 to cysteines and tagged these sites with maleimide derivative of terbium chelate (donor) and ATTO465 (acceptor) fluorophores (site 741 is shown in Fig. 1). The receptors were tagged with a 1:4 ratio of acceptor:donor, thus ensuring that the majority of the receptors probed have one acceptor per receptor (19). Labeling the same site on the four subunits allows the measurement of the intersubunit distance between the same sites on the four subunits.

The modified receptors were investigated by expression in either oocytes or HEK-293 cells, and their functionality was established by electrophysiology (Fig. 2 and Figs. S1–S3). For the LRET measurements, background labeling of inherent cysteines was reduced in oocytes by blocking with β-maleimidopropionic acid before the expression of AMPA receptor constructs. The preblocking procedure has been used in LRET investigations of potassium channels and increases the specificity of fluorophore labeling by ensuring that any background cysteines are blocked (19). The expression levels for the AMPA receptor constructs are too low to perform single-oocyte LRET measurements, and hence membrane preparations from several hundred oocytes were used. The same number of noninjected oocytes were used as control to remove any further nonspecific background. To establish that the LRET changes are not a function of the oocyte system, the ΔN*-GluR4-S741C construct also was investigated using HEK-293 cells. Preblocking does not reduce background in HEK-293 cells; therefore, to determine the background, a thrombin-recognition sequence was introduced on either side of the donor/acceptor site (ΔN*-GluR4-Th-S741C-Th). We therefore were able to determine the background LRET quantitatively by obtaining the lifetime after cleaving the fluorophore tagged to the receptor with the addition of thrombin (Fig. S4). Thus, the background obtained could be subtracted from the initial LRET signal to obtain the signal specific to the ΔN*-GluR4-Th-S741C-Th receptor.

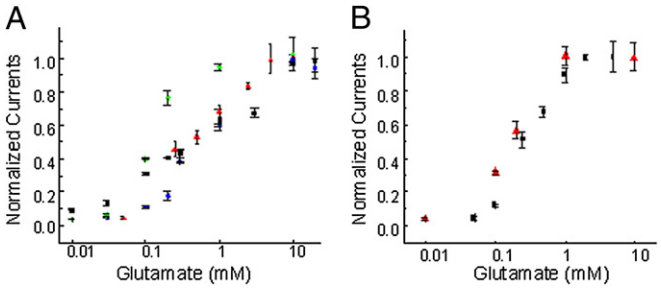

Fig. 2. Dose–response curve showing the dependence of the maximum current as a function of glutamate concentration. (*A*) ΔN-GluR4 receptors (red), ΔN*-GluR4-G740C (blue), ΔN*-GluR4-S741C (green), and ΔN*-GluR4-S742C (black) receptors expressed in oocytes with varying concentrations of glutamate in 100 μM cyclothiazide. (*B*) Wild-type GluR4-flip receptors (red) and ΔN*-GluR4-Th-S741C-Th receptors (black) expressed in HEK-293 cells. All currents were recorded in the presence of cyclothiazide and normalized to currents mediated by 10 mM glutamate.

LRET Investigations of the Receptors Stabilized Primarily in Closed Resting State, Open-Channel State, and Desensitized States. The LRET lifetimes were measured in the unligated state, in the presence of saturating concentrations of glutamate, and in the presence of saturating concentrations of glutamate and 100 μM cyclothiazide. The experiments also were performed in the presence of the L484Y mutation. The background was determined using labeled, noninjected oocytes or postthrombin digestion signal for HEK-293 cells and was subtracted to provide the final lifetimes (Fig. 3). To establish the state of the receptor, macroscopic currents were measured under the conditions for the LRET measurements. Consistent with previous reports on the AMPA receptors, the typical whole-cell currents for the ΔN*-GluR4-Th-S741C-Th expressed in HEK-293 cells show that the receptor exists primarily in the resting closed state in the

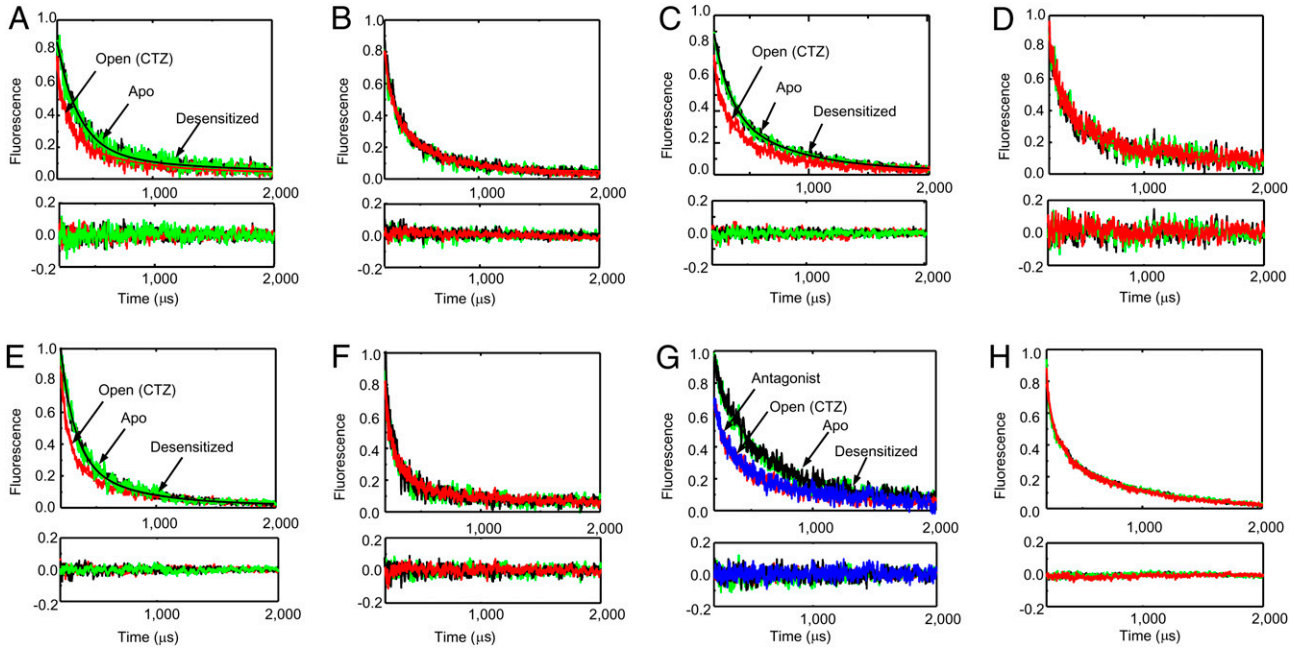

Fig. 3. The LRET lifetimes measured at 510 nm for donor:acceptor-tagged receptors. Lifetimes are shown for (*A*) ΔN*-GluR4-G740C, (*B*) ΔN*-GluR4-G740C-L484Y, (*C*) ΔN*-GluR4-S741C, (*D*) ΔN*-GluR4-S741C-L484Y, (*E*) ΔN*-GluR4-S742C, and (*F*) ΔN*-GluR4-S742C-L484Y receptors expressed in oocytes in the absence of agonists (black), with 10 mM glutamate (green), and with 10 mM glutamate in the presence of 100 μM cyclothiazide (red). Lifetimes after subtraction of the residual lifetimes upon thrombin digestion for (*G*) ΔN*-GluR4-Th-S741-Th and (*H*) ΔN*-GluR4-Th-S741-Th-L484Y receptors expressed in HEK-293 cells in the absence of agonists (black), with 10 mM glutamate (green), with 10 mM glutamate in the presence of 100 μM cyclothiazide (red), and in the presence of 200 nM antagonist ZK200775 (blue).

unligated state, in the desensitized state in the presence of saturating concentrations of glutamate, and in the open-channel state in the presence of saturating concentrations of glutamate and 100 μM cyclothiazide (Fig. S3). The LRET lifetimes studied under these conditions represent an average distance of the sites tagged with donor and acceptor fluorophore in the receptor primarily in the resting, desensitized, and open-channel state.

The receptors tagged with donor alone showed no significant changes in the three states and could be well represented by a single exponential decay (Fig. S5). The LRET lifetime for the donor-acceptor–tagged receptors ΔN*-GluR4-Th-S741C-Th expressed in HEK-293 cells as well as ΔN*-GluR4-S741C, ΔN*-GluR4-G740C, and ΔN*-GluR4-S742C expressed in oocytes can be fit with two exponentials (Fig. 3). The data with logarithmic y-scale are shown in Figs. S6 and S7. The faster lifetime (shortest distance) component represents ≈90% of the signal, and the distance for this lifetime is in the same range as the crystal structure distances (Table 1). The LRET distances in the open-channel dynamic form of the receptor are 20 Å, 19 Å (21 in HEK 293 cells), and 21 Å for sites 740, 741, and 742, respectively, and these distances are in reasonably good agreement with the corresponding crystal structure distances, which are 17 Å, 20 Å, and 22 Å (backbone nitrogen distances), respectively. The structure of the full-length AMPA receptor shows that the distances across the dimer for the same residues are in the range of 55–70 Å. Because the terbium chelate and ATTO465 donor-acceptor pair have an R_0 of 35 Å, the LRET efficiency for the distances of 55–70 Å is expected to be less than 0.05. Hence we do not expect to see any significant LRET from the residues across the dimer. The LRET data also suggests that the longer distance of 30–32 Å in the LRET measurements, which accounts for ≈10% of the signal, could arise from a minor structural conformation of the receptor that is not observed in the crystal structure or from background nonspecific labeling that cannot be subtracted.

The main component of the LRET signal shows an increase of 3–5 Å in the intersubunit distances for the sites 740, 741, and 742 within the dimer between the desensitized and open states of the receptor (Table 1). This increase in distance across the dimer upon transitioning from the open-channel state to the desensitized state is consistent with the current hypothesis that predicts a decoupling of the dimer interface upon desensitization. This distance change, however, is smaller than the 8 Å distance change observed between residue 741 in the structure of the isolated ligand-binding domain for the receptor stabilized in the open-channel state and the structure of the GluR2-S1S2-S729C mutant, which is thought to represent the desensitized state. The distance change might be shorter because the structure of the isolated ligand-binding domain, which is in the "desensitized" state, is artificially decoupled and could represent an extreme case that is more decoupled than the physiological desensitized state. Also, the distance change (between the open and desensitized states) in the LRET measurements might be shorter relative to the x-ray structures because the distances measured are an average of the dynamic form of the receptor primarily stabilized in a given state, not the distances in one specific structure. Additionally, the single-channel recordings show that, although the channel is stabilized in the open-channel state for at least 80% of the time in the presence of cyclothiazide (Fig. S1) and for more than 95% of the time in the open-channel state in the L493Y mutant protein in the presence of cyclothiazide, the channel fluctuates to the closed-channel state for the remaining 5–20% of the time, and these fluctuations occur in the millisecond time scale (Fig. S1). Because we used LRET measurements, a significant fraction of these fluctuations occurred in the time scale of the luminescence decay, and hence the lifetimes provide only an average of the two states. Thus the shorter distance changes observed in the LRET investigations could reflect this limitation in the LRET investigations. Additionally, electrophysiological measurements have shown that there may be

Table 1. Fluorescence lifetimes and distances

Protein	Ligand/state	Donor lifetime (μs)	Sensitized emission lifetime (μs)	Distance (Å)
ΔN*-GluR4-G740C	Apo/resting	1526 ± 50	188 ± 12	25 ± 0.3
			535 ± 15	32 ± 0.3
ΔN*-GluR4-G740C	Glu/desensitized	1510 ± 45	173 ± 10	25 ± 0.3
			534 ± 18	32 ± 0.3
ΔN*-GluR4-G740C	Glu+CTZ/open	1534 ± 45	73 ± 10	21 ± 0.5
			439 ± 15	30 ± 0.3
ΔN*-GluR4-G740C-L484Y	Apo	1841 ± 50	63 ± 5	20 ± 0.3
			336 ± 18	27 ± 0.3
ΔN*-GluR4-G740C-L484Y	Glu	1845 ± 60	67 ± 3	20 ± 0.2
			357 ± 20	28 ± 0.3
ΔN*-GluR4-G740C-L484Y	Glu+CTZ/open	1845 ± 60	61 ± 8	20 ± 0.5
			444 ± 21	29 ± 0.3
ΔN*-GluR4-S741C	Apo/resting	1682 ± 50	132 ± 9	23 ± 0.3
			595 ± 23	32 ± 0.3
ΔN*-GluR4-S741C	Glu/desensitized	1686 ± 60	126 ± 10	23 ± 0.3
			522 ± 20	31 ± 0.3
ΔN*-GluR4-S741C	Glu+CTZ/open	1612 ± 60	60 ± 7	20 ± 0.4
			367 ± 15	29 ± 0.3
ΔN*-GluR4-S741C-L484Y	Apo	1877 ± 45	53 ± 9	19 ± 0.6
			542 ± 19	30 ± 0.3
ΔN*-GluR4-S741C-L484Y	Glu	1820 ± 45	55 ± 10	20 ± 0.6
			565 ± 17	31 ± 0.3
ΔN*-GluR4-S741C-L484Y	Glu+CTZ/open	1818 ± 50	51 ± 10	19 ± 0.6
			584 ± 15	31 ± 0.3
ΔN*-GluR4-Th-S741C-Th	Apo/resting	1578 ± 45	188 ± 13	25 ± 0.3
			535 ± 16	31 ± 0.3
ΔN*-GluR4-Th-S741C-Th	Glu/desensitized	1505 ± 45	174 ± 4	25 ± 0.2
			534 ± 20	32 ± 0.3
ΔN*-GluR4-Th-S741C-Th	Glu+CTZ/open	1579 ± 55	73 ± 3	21 ± 0.2
			439 ± 15	30 ± 0.3
ΔN*-GluR4-Th-S741C-Th	ZK200775	1679 ± 45	77 ± 5	21 ± 0.2
			489 ± 15	30 ± 0.3
ΔN*-GluR4-Th-S741C-Th-L484Y	Apo	1609 ± 60	70 ± 1	21 ± 0.1
			588 ± 7	32 ± 0.3
ΔN*-GluR4-Th-S741C-Th-L484Y	Glu	1565 ± 55	70 ± 1	21 ± 0.1
			582 ± 9	32 ± 0.3
ΔN*-GluR4-Th-S741C-Th-L484Y	Glu+CTZ/open	1579 ± 50	70 ± 1	21 ± 0.1
			558 ± 8	32 ± 0.3
ΔN*-GluR4-S742C	Apo/resting	1704 ± 60	124 ± 7	23 ± 0.3
			596 ± 22	32 ± 0.4
ΔN*-GluR4-S742C	Glu/desensitized	1730 ± 60	118 ± 6	23 ± 0.2
			517 ± 15	30 ± 0.3
ΔN*-GluR4-S742C	Glu+CTZ/open	1682 ± 55	62 ± 5	20 ± 0.3
			444 ± 15	29 ± 0.3
ΔN*-GluR4-S742C-L484Y	Apo	1557 ± 45	66 ± 5	21 ± 0.3
			464 ± 15	30 ± 0.3
ΔN*-GluR4-S742C-L484Y	Glu	1517 ± 45	67 ± 5	21 ± 0.3
			477 ± 15	31 ± 0.3
ΔN*-GluR4-S742C-L484Y	Glu+CTZ/open	1509 ± 45	64 ± 5	21 ± 0.3
			446 ± 15	30 ± 0.3

CTZ, cyclothiazide; Glu, glutamate.

more than one desensitized form; some of these states may be too close to resolve, and the distance measured would be an average representation of these states.

Dimer Interface in the Resting State of the Receptor and the Mechanism of Activation in AMPA Receptors. The LRET lifetimes and the intersubunit distances for all the constructs without the L484Y mutation show that the Apo state distances are the same as that of the desensitized state distances, although the Apo state distances are significantly longer (3–5 Å) than those observed when the receptor is in the open-channel state. The longer intersubunit distances suggest that in the resting unligated state of the receptor the dimer interface is decoupled and not preformed as observed in the crystal structures of the isolated ligand-binding domain. The decoupling the interface in the unligated form of the AMPA receptor is consistent with the crosslinking measurements of the GluR2-S729C mutant (20). These studies show disulphide bond formation at the 729 site in the resting and desensitized state, reduced levels of disulphide bond formation in the antagonist-bound form, and no disulphide bond formation in L484Y-mutant background. The crosslinking results indicate that stabilization of interactions at the upper lobe of the receptor by the L484Y mu-

tation block the ability to form the disulphide bond at the 729 site; conversely, the formation of the disulphide bond in the resting unligated state of the protein was thought to be caused by breakage of the interactions at the upper lobe of the dimer interface. Thus the unligated state of the receptor was believed to have a dynamic interface with spontaneous breakage of the interactions in the upper lobe of the ligand-binding domain.

The LRET lifetimes for the L484Y-mutant proteins also are consistent with the crosslinking experiments that show a stabilization of the upper lobes of the agonist-binding domain (20). The LRET investigations show that the distances are similar in the Apo state, glutamate-bound state, and glutamate-bound state in the presence of cyclothiazide for the L484Y-mutant receptor. Additionally, the intersubunit distance in the L484Y mutant within the dimer is similar to that observed for the open-channel form of AMPA receptor stabilized by cyclothiazide. These results indicate that, in the L484Y-mutant protein, the dimer interface is preformed in the resting unligated state of the protein. Additionally, the studies with the L484Y mutation indicate that preformation of the dimer interface is not sufficient to drive activation, because glutamate binding is required for activation of L484Y-mutant receptor. However, the preformation of the dimer interface in the resting state of the L484Y mutant is expected to contribute to the energetics of channel opening and agonist binding. This contribution is consistent with the lower EC_{50} values determined in the L484Y-mutant proteins relative to wild-type receptors for glutamate activation.

LRET measurements were performed using the AMPA receptor in complex with competitive antagonist ZK200775 (Fig. 3), allowing a direct comparison of the LRET-based distances and the recent structure of the full-length AMPA receptor (18). The distance measured by LRET, 21 Å, was similar to that observed in the coupled states of the AMPA receptor and to the 20-Å distances observed in the full-length AMPA receptor structure. These results further confirm that the decoupling of the dimer interface in the resting unligated receptor is caused by the dynamic nature of this receptor and not by the open-cleft form of the receptor as seen in the competitive antagonist ZK200775-bound form of the receptor.

The mechanism based on the LRET investigations is shown in Fig. 4. These studies show that the dimer interface is decoupled in the resting state, and the agonist binding not only induces cleft closure within the domain but also allows the formation of the dimer interface. The formation of the contact at the interface between the subunits in the dimer could transiently stabilize the open-channel form. Furthermore, as previously hypothesized, the dimer interface decouples in the continued presence of the agonists, possibly because of the stress induced by the transmembrane segments leading to desensitization (Fig. 4). The dynamic uncoupled state of the dimer interface in the resting state is relevant in terms of the primary role of agonist-mediated receptor activation and desensitization and also could play an important role in mediating effects of modulators. For instance, a mechanism similar to that observed in the L484Y mutant could underlie the modulatory action of the transmembrane AMPA-receptor regulatory proteins, such as stargazin, so that these proteins could facilitate assembly of the dimer interface and thereby promote receptor activation. Furthermore, the role of the dimer interface is not limited to the AMPA subtype of the glutamate receptors. Recent investigations on the NMDA receptor subtype of the glutamate receptors show that modulators such as Zn^{2+} and protons that bind to the N-terminal domain of the receptor modulate the activation and desensitization through the interactions at the dimer interface in the ligand-binding domain. Hence, it is likely that the resting state of the receptor is altered in the presence of the N-terminal domain and modulators that bind to this domain.

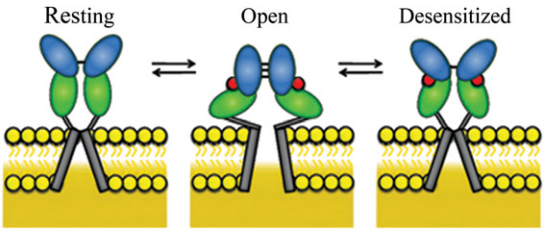

Fig. 4. Proposed mechanism showing changes in the ligand-binding domain associated with the resting state, activation, and desensitization. Agonist binding to the ligand-binding domain induces cleft closure in the ligand-binding domain, pulling apart the linker to the channel segments opening the channel (activation). The open-channel form is transiently stabilized through transiently formed dimer interface interactions at the ligand-binding domain. Stress on the linker domain eventually results in decoupling of the ligand-binding domain dimer interface interactions, leading to channel closure (desensitization).

Methods

Modifications Introduced in the GluR4 AMPA Receptor. For studying the conformational changes in the ligand-binding domain of the AMPA receptor, we used a modified GluR4 subunit of the AMPA receptor lacking the N-terminal domain and with the two accessible cysteines (C426, C529) on the extracellular side mutated to serines, producing a modified AMPA receptor with no accessible cysteines. A cysteine was introduced at site G740, S741, or S742 to create modified AMPA receptors (ΔN*-GluR4-G740C, ΔN*-GluR4-S741C, and ΔN*-GluR4-S742C). A thrombin cleavage site was added on each side of the S741C mutant to create ΔN*-GluR4-Th-S741C-Th.

Mutant Plasmid Preparation. The plasmid for the GluR4-flip receptor with the first 402 residues to the N-terminal domain deleted was provided by K. Keinanen (University of Helsinki, Helsinki, Finland). For the ΔN*-GluR4-Th-S741C-Th two thrombin cleavage sites (LVPRGS) were inserted before and after a cysteine at site 741. Mutations in the plasmids were introduced using the Stratagene QuikChange site-directed mutagenesis kit. The integrity of the final constructs was verified by sequencing the coding region.

Expression of ΔN*-AMPA receptor. Oocytes were prepared and injected with mutant RNA as previously performed (21). After injection, the oocytes were incubated for 48 h at 12 °C and then were prelabeled with β-maleimidopropionic acid for 1 h to block inherent cysteines (21). The blocked oocytes were held at 18 °C for 24–36 h, allowing receptor expression. HEK-293 cells were cultured as described by Du et al. (22). Transfected cells were allowed to grow for 24–36 h before use.

Tagging of the ΔN*-AMPA receptor. At the end of 24–36 h, the receptors were labeled with a 4:1 ratio of donor:acceptor, thus generating a probe on the four subunits of an AMPA receptor, and the intersubunit distance was measured by studying the LRET lifetimes. Specifically, 2 μM thiol-reactive terbium chelate (donor) and 0.5 μM ATTO465 maleimide (acceptor) in extracellular buffer or storage solution were added to the cells or oocytes for 1 h, and excess fluorophore then was washed away. The membrane preparations from oocytes obtained by lysis were used for single-channel recordings (Fig. S1) and fluorescence measurements as per Gonzalez et al. (21). To obtain the background LRET for ΔN*-GluR4-Th-S741C-Th, the cells used for the LRET measurements were incubated at room temperature with 3 U of thrombin (Calbiochem). Background LRET was measured 3 h after the addition of the thrombin and subtracted from the total LRET signal to obtain the LRET signal from ΔN*-GluR4-Th-S741C-Th.

Fluorescence Spectroscopy. ATTO465 maleimide was purchased from Sigma-Aldrich, and the terbium chelate was purchased from Invitrogen Corp. The fluorescence measurements were performed using a cuvette-based fluorescence lifetime spectrometer, QuantaMaster model QM3-SS (Photon Technology International). The excitation source was a high-power pulsed xenon lamp. Emitted light was collected and passed through a monochromator to a detector. The sample was held at 15 °C with a Peltier temperature controller (Photon Technology International). At least two independent sets of experiments were performed for each mutant receptor. Each experiment is reported as an average of three measurements for a given state, with each

measurement having an average of 99 pulses from the flash lamp. The experiments were performed by adding glutamate and cyclothiazide consecutively to the same sample. Data were collected using Fluorescan software (Photon Technology International) and analyzed using Origin software (OriginLab Corp).

LRET lifetimes were obtained by studying the sensitized emission at 510 nm for ATTO465, and the donor-only lifetimes were collected at 488 nm. The donor-only and acceptor-only fluorophore samples probed at 510 nm are shown in Fig. S8. There is no background signal from the donor-only and acceptor-only sample at this wavelength. Additionally, no significant effects were observed on the absorption spectrum of ATTO465 because of the addition of glutamate as well as cyclothiazide (Fig. S9). The LRET lifetimes were fit by nonlinear regression analysis of the data to Eq. **1**:

$$y = y_0 + \sum A * e^{-\frac{t}{\tau}} \quad [1]$$

where y_0 is background noise, A is the amplitude, and τ is the lifetime.

Distance Calculations Based on Lifetimes. The distance between the donor:acceptor fluorophores was determined measuring the time constants of donor fluorescence decay in the absence (τ_D) and sensitized emission of the acceptor caused by energy transfer from the donor (τ_{DA}) and using Forster's equation (Eq. **2**).

$$R = R_0 \left(\frac{\tau_{DA}}{\tau_D - \tau_{DA}} \right)^{1/6} \quad [2]$$

The R_o for terbium chelate and ATTO465 was calculated using the overlap integral J. The overlap integral J was calculated using Eq. **3**:

$$J = \frac{\sum_i F_D(\lambda_i) * \varepsilon_A(\lambda_i) * \lambda_i^4}{\sum_i F_D(\lambda_i)} \quad [3]$$

where $F_D(\lambda)$ is the fluorescence spectrum of terbium chelate, $\varepsilon_A(\lambda)$ is the absorption spectrum of ATTO465, and λ is the wavelength. The calculations were performed using an Excel spreadsheet (Microsoft), and the value of J was determined to be $1.89*10^{14}$ $M^{-1}cm^{-1}nm^4$. Using this value for J, R_0 then was calculated using Eq. **4**:

$$R_0^6 = \frac{8.785*10^{-5}*\kappa^2*\varphi_D*J}{n^4} \quad [4]$$

where κ is the orientation factor, φ is the quantum yield of terbium chelate, and n is the refractive index. Using 2/3 as the value for κ (23), 0.73 as the value of φ for terbium chelate (24), and 1.3 as the value for n, R_0 was determined to be 35 Å. The error in the distances was calculated using propagation of errors.

Electrophysiological Measurements. For electrophysiological characterization, the cells or oocytes expressing the mutant receptors were labeled with the fluorophore for 1 h and then were rinsed before recordings. Two-electrode voltage-clamp and whole-cell current recordings were performed as previously described (21, 22).

ACKNOWLEDGMENTS. This work was supported by National Institutes of Health Grant R01GM073102. J.G. was supported by National Institutes of Health National Research Service Award GM082023-01.

1. Hollmann M, Heinemann S (1994) Cloned glutamate receptors. *Annu Rev Neurosci* 17: 31–108.
2. Nakanishi S, Masu M (1994) Molecular diversity and functions of glutamate receptors. *Annu Rev Biophys Biomol Struct* 23:329–348.
3. Madden DR (2002) The structure and function of glutamate receptor ion channels. *Nat Rev Neurosci* 3:91–101.
4. Mayer ML (2005) Glutamate receptor ion channels. *Curr Opin Neurobiol* 15:282–288.
5. Mayer ML (2006) Glutamate receptors at atomic resolution. *Nature* 440:456–462.
6. Oswald RE, Ahmed A, Fenwick MK, Loh AP (2007) Structure of glutamate receptors. *Curr Drug Targets* 8:573–582.
7. Armstrong N, Gouaux E (2000) Mechanisms for activation and antagonism of an AMPA-sensitive glutamate receptor: Crystal structures of the GluR2 ligand binding core. *Neuron* 28:165–181.
8. Gouaux E (2004) Structure and function of AMPA receptors. *J Physiol* 554:249–253.
9. Armstrong N, Jasti J, Beich-Frandsen M, Gouaux E (2006) Measurement of conformational changes accompanying desensitization in an ionotropic glutamate receptor. *Cell* 127:85–97.
10. Armstrong N, Sun Y, Chen GQ, Gouaux E (1998) Structure of a glutamate-receptor ligand-binding core in complex with kainate. *Nature* 395:913–917.
11. Jin R, Horning M, Mayer ML, Gouaux E (2002) Mechanism of activation and selectivity in a ligand-gated ion channel: Structural and functional studies of GluR2 and quisqualate. *Biochemistry* 41:15635–15643.
12. Hogner A, et al. (2002) Structural basis for AMPA receptor activation and ligand selectivity: Crystal structures of five agonist complexes with the GluR2 ligand-binding core. *J Mol Biol* 322:93–109.
13. McFeeters RL, Oswald RE (2002) Structural mobility of the extracellular ligand-binding core of an ionotropic glutamate receptor. Analysis of NMR relaxation dynamics. *Biochemistry* 41:10472–10481.
14. Sun Y, et al. (2002) Mechanism of glutamate receptor desensitization. *Nature* 417: 245–253.
15. Jin R, Banke TG, Mayer ML, Traynelis SF, Gouaux E (2003) Structural basis for partial agonist action at ionotropic glutamate receptors. *Nat Neurosci* 6:803–810.
16. Jin R, et al. (2009) Crystal structure and association behaviour of the GluR2 amino-terminal domain. *EMBO J* 28:1812–1823.
17. Gill A, Birdsey-Benson A, Jones BL, Henderson LP, Madden DR (2008) Correlating AMPA receptor activation and cleft closure across subunits: Crystal structures of the GluR4 ligand-binding domain in complex with full and partial agonists. *Biochemistry* 47:13831–13841.
18. Sobolevsky AI, Rosconi MP, Gouaux E (2009) X-ray structure, symmetry and mechanism of an AMPA-subtype glutamate receptor. *Nature* 462:745–756.
19. Cha A, Snyder GE, Selvin PR, Bezanilla F (1999) Atomic scale movement of the voltage-sensing region in a potassium channel measured via spectroscopy. *Nature* 402: 809–813.
20. Plested AJ, Mayer ML (2009) AMPA receptor ligand binding domain mobility revealed by functional cross linking. *J Neurosci* 29:11912–11923.
21. Gonzalez J, Rambhadran A, Du M, Jayaraman V (2008) LRET investigations of conformational changes in the ligand binding domain of a functional AMPA receptor. *Biochemistry* 47:10027–10032.
22. Du M, Reid SA, Jayaraman V (2005) Conformational changes in the ligand-binding domain of a functional ionotropic glutamate receptor. *J Biol Chem* 280:8633–8636.
23. Haas E, Katchalski-Katzir E, Steinberg IZ (1978) Effect of the orientation of donor and acceptor on the probability of energy transfer involving electronic transitions of mixed polarization. *Biochemistry* 17:5064–5070.
24. Xiao M, Selvin PR (2001) Quantum yields of luminescent lanthanide chelates and far-red dyes measured by resonance energy transfer. *J Am Chem Soc* 123:7067–7073.